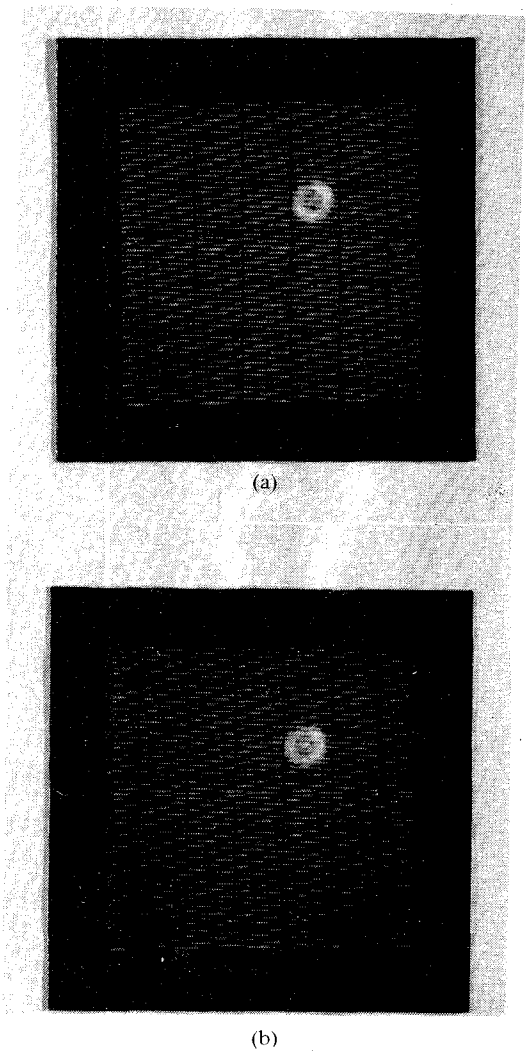

Fig. 4. The reconstructed microwave images from slices of (a) $\rho(\boldsymbol{p})/p$ and (b) $\Gamma(\boldsymbol{p})$ data measured in the frequency range 4–10 GHz.

position of the specular region when the T/R unit is at the other side. Therefore, the $\Gamma(\boldsymbol{p})$ data shown in Fig. 2(b) are symmetrical not only to $\theta = 45°$ but also to the center, whereas $\rho(\boldsymbol{p})/p$ data are symmetrical to $\theta = 45°$ only. However, they both yield images with the same feature showing the cylinder profile formed by specular regions as given in Fig. 4(a) and (b).

IV. Conclusions

In this paper, we have discussed the microwave images of a metallic convex object under physical optics approximations. It is shown that the image reconstructed from Bojarski's identity is the "edge-enhanced" version of the object characteristic function of the distribution of specular reflection regions. The same image can also be reconstructed from the range-normalized scattered far field using one-dimensional Fourier inversion and a back-projection algorithm.

References

[1] R. M. Lewis, "Physical optics inverse diffraction," *IEEE Trans. Antennas Propagat.*, vol. AP-24, pp. 308–314, May 1969.

[2] N. N. Bojarski, "A survey of physical optics inverse scattering identity," *IEEE Trans. Antennas Propagat.*, vol. AP-30, pp. 980–989, Sept. 1982.

[3] N. H. Farhat, C. L. Werner, and T. H. Chu, "Prospects for three-dimensional projective and tomographic imaging radar network," *Radio Sci.*, vol. 19, no. 5, pp. 1347–1355, Sept. 1984.

[4] W-M. Boerner, C. M. Ho, and B. Y. Foo, "Use of Radon's projection theory in electromagnetic inverse scattering," *IEEE Trans. Antennas Propagat.*, vol. AP-29, pp. 336–341, Mar. 1981.

[5] G. T. Ruck, D. E. Barrick, W. D. Stuart, and C. K. Krichbaum, *Radar Cross Section Handbook*. New York: Plenum, 1970.

[6] G. T. Herman, *Image Reconstruction from Projections — Implementation and Applications*. New York: Springer-Verlag, 1979.

[7] A. Papoulis, *Systems and Transforms with Applications in Optics*. New York: McGraw-Hill, 1968.

[8] D. C. Munson and J. L. C. Sanz, "Image reconstruction from frequency-offset Fourier data," *Proc. IEEE*, vol. 72, pp. 661–669, June 1984.

The Input Impedance of a Hollow-Probe-Fed, Semi-Infinite Rectangular Waveguide

JOHN M. ROLLINS AND JOHN M. JAREM, MEMBER, IEEE

Abstract **— Image theory is used to determine the input impedance of a coaxial feed in a short-circuited, semi-infinite rectangular waveguide. The analysis presented here is applicable to hollow antenna probes of variable height and lends itself well to accurate numerical evaluation. The numerical results are compared to results obtained from other methods and show the efficacy of using image theory to determine the waveguide input impedance.**

I. Introduction

A common problem in many microwave applications is the determination of the input impedance of a coaxially fed antenna probe in a rectangular waveguide. Several closed-form solutions [1], [2] of varying accuracy have been developed for the case where the waveguide is infinite in the forward and reverse directions of propagation. Considerable effort has also been expended in achieving input-impedance expressions for the case where one of the waveguide arms has been terminated with a short-circuiting plate, resulting in a semi-infinite waveguide geometry (Fig. 1).

In determining the input impedance of an infinite waveguide, one method, which has been pursued by Williamson [1], is the use of image theory to develop expressions for the electric and magnetic fields in the vicinity of the coaxial aperture. In his analysis, Williamson assumes perfect conductivity for the waveguide walls and shows that the system is equivalent to an infinite array of image sources which are treated as if they existed in free space and contributed to the fields affecting the primary waveguide feed (parent source). Each source, real or image, radiates fields which are due to a magnetic surface current in the annular region of its aperture and an electric surface current which flows on the surface of the probe. For the infinite waveguide shown in Fig. 1, Williamson obtains an expression for the admittance using a hollow probe of arbitrary height [1].

The introduction of a short circuit plate down the waveguide at a distance u from the center of the probe results in two arrays of probe and aperture images parallel to each other and separated by a distance $2u$. Each image is a source of radiating fields which are felt at the coaxial aperture and ultimately affect the input

Manuscript received October 30, 1987; revised June 28, 1988. This work was supported by Sandia National Laboratories, Albuquerque, NM 87185, under Contract 01-3817.

The authors are with the Department of Electrical Engineering, University of Texas at El Paso, El Paso, TX 79968.

IEEE Log Number 8927786.

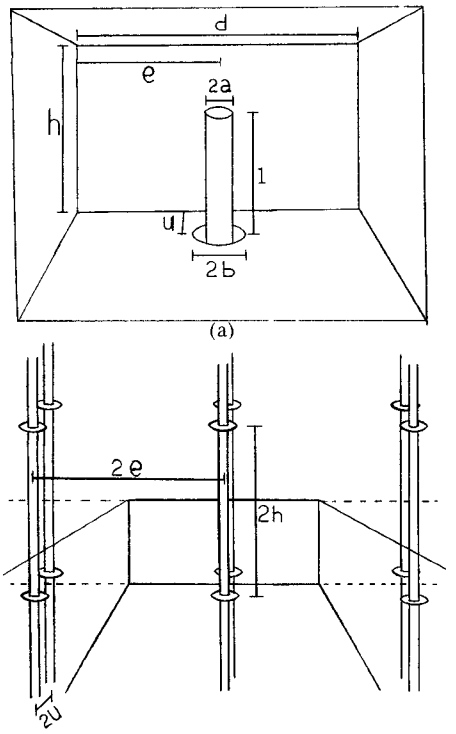

Fig. 1. (a) Waveguide system and dimensions. (b) Infinite arrays; probe spans height.

impedance of the waveguide. Axial symmetry is assumed for the current distributions of each source ($a/d < 0.04$; see [8]). In order to obtain expressions for the total electromagnetic fields at the aperture, we must obtain an array factor which summarizes the superposition of average values of the field contributions from each of the image sources.

This array factor involves four terms, two representing the images in the plane coincident with the parent source and two representing the sources in the short circuit image plane. The array factors are calculated following Williamson's procedure outlined in [3]. The resulting expressions may be used in an admittance formula derived by Williamson [1] (for an infinite waveguide). A modified expression representing the semi-infinite case results and is given by

$$Y = Y_c - \sum_{p=0}^{pm} e_p^{pm}(-1)^p \sum_{m=0}^{\infty} Y_m(-1)^m J_{2p}(mc)$$

where the waveguide-height probe admittance is

$$Y_c = -\left(2\pi j/\left(Z_0 kh \ln^2(b/a)\right)\right)\{\ln(b/a) + (\pi/2)(Y_0(ka)J_0(kb) - Y_0(kb)J_0(ka))$$

$$*\left(\frac{J_0(kb)}{J_0(ka)} + j\frac{J_0(kb)Y_0(ka) - J_0(ka)Y_0(kb)}{J_0(ka)\,\mathrm{SC}*(ka, kd, ku, e/d)}\right)$$

$$-\sum_{m=1}^{\infty}\left(2/q_m^2\right)\Bigg[\ln(b/a) + (K_0(q_m kb)I_0(q_m ka) - K_0(q_m ka)I_0(q_m kb))$$

$$*\left[\frac{I_0(q_m kb)}{I_0(q_m ka)} - \frac{I_0(q_m kb)K_0(q_m ka) - I_0(q_m ka)K_0(q_m kb)}{I_0(q_m ka)\,\mathrm{SC}(q_m ka, q_m kd, q_m ku, e/d)}\right]\Bigg]\Bigg\}$$

where $q_m^2 = (m\pi/kh)^2 - 1$ and $c = \pi(h-l)/h$. In addition,

$$Y_m = \left(2\pi j/\left(Z_0 kh \ln(b/a)\right)\right)$$

$$\cdot\left[\frac{J_0(kb)}{J_0(ka)} - 1 + j\frac{J_0(kb)Y_0(ka) - J_0(ka)Y_0(kb)}{J_0(ka)\,\mathrm{SC}*(ka, kd, ku, e/d)}\right.$$

$$+\sum_{m=1}^{\infty}\frac{2}{q_m^2}\left[1 - \frac{I_0(q_m kb)}{I_0(q_m ka)}\right.$$

$$\left.\left.+\frac{I_0(q_m kb)K_0(q_m ka) - I_0(q_m ka)K_0(q_m kb)}{I_0(q_m ka)\,\mathrm{SC}(q_m ka, q_m kd, q_m ku, e/d)}\right]\right].$$

SC and SC* are the array factors which have been modified by the addition of the short circuit plate. Hence, they include contributions from the second array of images and are given by

$$\mathrm{SC}(q_m ka, q_m kd, q_m ku, e/d)$$

$$= K_0(q_m ka) + I_0(q_m ka)$$

$$\cdot\left[\sum_{\substack{n=-\infty \\ n\neq 0}}^{\infty} K_0(2|n|q_m kd) - \sum_{n=-\infty}^{\infty} K_0(2|nd+e|q_m k)\right.$$

$$+\sum_{n=-\infty}^{\infty}\left(K_0\left(2\sqrt{(nd+e)^2+u^2}\,q_m k\right)\right.$$

$$\left.\left.-K_0\left(2\sqrt{(nd)^2+u^2}\,q_m k\right)\right)\right]$$

$$\mathrm{SC}*(ka, kd, ku, e/d)$$

$$= H_0^{(2)}(ka) + J_0(ka)$$

$$\cdot\left[\sum_{\substack{n=-\infty \\ n\neq 0}}^{\infty} H_0^{(2)}(2|n|kd) - \sum_{n=-\infty}^{\infty} H_0^{(2)}(2|nd+e|k)\right.$$

$$+\sum_{n=-\infty}^{\infty}\left(H_0^{(2)}\left(2\sqrt{(nd+e)^2+u^2}\,k\right)\right.$$

$$\left.\left.-H_0^{(2)}\left(2\sqrt{(nd)^2+u^2}\,k\right)\right)\right].$$

Note that $\mathrm{SC}*(A, B, C, D) = (2j/\pi)\mathrm{SC}(jA, jB, jC, D)$.

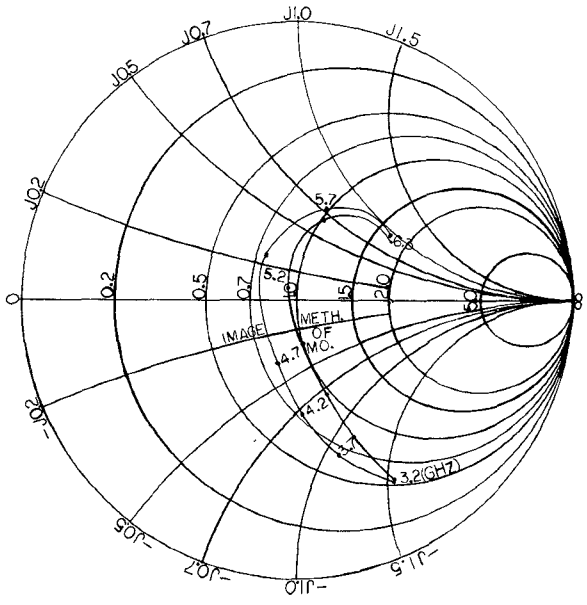

Fig. 2. Method-of-moments results using a solid probe are compared to those for image theory based on a hollow-probe configuration. $a = 0.0635$ cm, $d = 5\,704$ cm, $h = 2\,880$ cm, $l = 1.440$ cm, $u = 1\,920$ cm, $e/d = 0.5$, relative permittivity: 1.0, (50 Ω coaxial line).

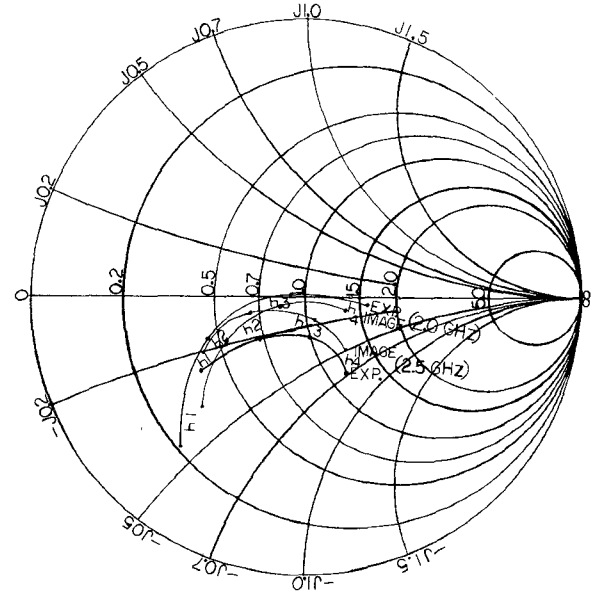

Fig. 3. Image theory results for a hollow probe are compared to experimental results (solid probe). $a = 0.1778$ cm, $d = 5.715$ cm, $h = 2.223$ cm, $u = 1.524$ cm, $e/d = 0.5$, relative permittivity: 3.75, for probe heights. $h_1 = 1.270$ cm, $h_2 = 1.524$ cm, $h_3 = 1.778$ cm, $h_4 = 2.032$ cm (50 Ω coaxial line).

In the above expressions, Y_c represents the input admittance of a waveguide whose probe extends to the top. The parameter k is the wavenumber, Z_0 is the free-space intrinsic impedance, and a, b, d, e, u, and h are the waveguide dimensions as shown in Fig. 1. The e_p and Y_m coefficients, which have been derived by Williamson [1] using the method of moments, describe the effect of electric fields above a variable-height probe on the input admittance of the waveguide. As in [1], convergence of the series giving the e_p coefficients is fairly rapid due to the diagonal nature of the matrix associated with it. Negligible accuracy is gained in setting the order greater than 4.

II. Numerical Results

A numerical evaluation of the admittance expression was made and the results were compared to data available from other sources. In the first case (see Fig. 2), the method-of-moments algorithm developed by Jarem [2] generated data for comparison. His program, based on a solid-probe configuration, produced results which differed moderately from those of the image method. The amount of the disparity is believed to be due to the difference between the fields emanating from a hollow probe and a solid one [7]. (The internal current which flows in a hollow probe is not present in a solid one and can have a small effect on the outside fields.)

A comparison was also made with experimental results [2] over a range of two frequencies and four probe heights (see Fig. 3). The experimental waveguide used a solid probe, and a moderate displacement between the image theory solution and the experimental results is seen to occur.

The results shown in Figs. 2 and 3, though displaying moderate differences between alternative data, suggest a fair degree of efficacy in using this image theory method for semi-infinite waveguide input impedance determinations, even if a solid probe is used.

III. Conclusions

The method of images as developed by Williamson can be used as an alternative approach in determining the input impedance of a hollow-probe-fed, semi-infinite rectangular waveguide. Further assessment of this method could best be facilitated through experimental comparison where an actual hollow probe is used.

Acknowledgment

The authors would like to thank Dr. W. Schaedla and Dr. W. Brock, who supervised the academic and financial support from Sandia. Also greatly appreciated is the summary of research publications provided by Dr. A. G. Williamson regarding his research on this topic. His techniques formed the basis for the analysis in this paper and provided a unique and dependable alternative for waveguide research at the University of Texas at El Paso.

References

[1] A. G. Williamson, "Coaxially fed, hollow probe in a rectangular waveguide," *Proc. Inst. Elec. Eng.*, vol 132, pt. H, pp 273–285, 1985.

[2] J. M. Jarem, "A multi-filament method of moments solution for the input impedance of a probe-excited semi-infinite waveguide," *IEEE Trans. Microwave Theory Tech*, vol. MTT-35, Jan. 1987.

[3] R. E. Collin, *Field Theory of Guided Waves* New York: McGraw-Hill, 1960.

[4] M J. Al-Hakkak, "Experimental investigation of the input impedance characteristics of an antenna in a rectangular waveguide," *Electron. Lett.*, vol. 5, no 21, pp. 513–514, Oct 16, 1969.

[5] A. G. Williamson, "Analysis and modelling of a single-post waveguide mounting structure," *Proc. Inst Elec. Eng.*, vol 129, pt. H, pp. 271–277, 1982.

[6] A. G. Williamson, "Analysis and modelling of a coaxial-line rectangular waveguide junction," *Proc. Inst. Elec Eng.*, vol 129, pt. H, pp. 262–270. 1982.

[7] O. Einarson, "A comparison between tube-shaped and solid cylinder antennas," *IEEE Trans. Antennas Propagat.*, vol AP-14, pp. 31–37, 1966.

[8] A. G. Williamson, "Variable-length cylindrical post in a rectangular waveguide," *Proc. Inst. Elec. Eng.*, vol. 133, pt H, no 1, pp. 1–9, Feb. 1986.